A 300-year record of sedimentation in a small tilled catena in Hungary based on $\delta^{13}C$, $\delta^{15}N$, and C/N distribution

Gergely Jakab, [1✉,2]

Email jakab.gergely@csfk.mta.hu

István Hegyi, [3]

Michael Fullen, [4]

Judit Szabó, [1]

Dóra Zacháry, [1]

Zoltán Szalai, [1,2]

[1] Geographical Institute, Research Centre for Astronomy and Earth Sciences Hungarian Academy of Sciences, Budaörsi út 45, Budapest, 1112 Hungary AQ1

[2] Department of Environmental and Landscape Geography, Eötvös Loránd University, Pázmány P. sétány 1/c, Budapest, 1117 Hungary

[3] Institute for Geological and Geochemical Research, Research Centre for Astronomy and Earth Sciences, Hungarian Academy of Sciences, Budaörsi út 45, Budapest, 1112 Hungary

[4] Faculty of Science and Engineering, The University of Wolverhampton, Wolverhampton, WV1 1LY UK

Received: 25 July 2017 / Accepted: 19 December 2017

Abstract

Purpose

Soil erosion is one of the most serious hazards that endanger sustainable

food production. Moreover, it has marked effects on soil organic carbon (SOC) with direct links to global warming. At the same time, soil organic matter (SOM) changes in composition and space could influence these processes. The aim of this study was to predict soil erosion and sedimentation volume and dynamics on a typical hilly cropland area of Hungary due to forest clearance in the early eighteenth century.

Materials and methods

Horizontal soil samples were taken along two parallel intensively cultivated complex convex-concave slopes from the eroded upper parts at mid-slope positions and from sedimentation in toe-slopes. Samples were measured for SOC, total nitrogen (TN) content, and SOM compounds ($\delta^{13}C$, $\delta^{15}N$, and photometric indexes). They were compared to the horizons of an in situ non-eroded profile under continuous forest. On the depositional profile cores, soil depth prior to sedimentation was calculated by the determination of sediment thickness.

Results and discussion

Peaks of SOC in the sedimentation profiles indicated thicker initial profiles, while peaks in C/N ratio and $\delta^{13}C$ distribution showed the original surface to be ~ 20 cm lower. Peaks of SOC were presumed to be the results of deposition of SOC-enriched soil from the upper slope transported by selective erosion of finer particles (silts and clays). Therefore, changes in $\delta^{13}C$ values due to tillage and delivery would fingerprint the original surface much better under the sedimentation scenario than SOC content. Distribution of $\delta^{13}C$ also suggests that the main sedimentation phase occurred immediately after forest clearance and before the start of intense cultivation with maize.

Conclusions

This highlights the role of relief in sheet erosion intensity compared to intensive cultivation. Patterns of $\delta^{13}C$ indicate the original soil surface, even in profiles deposited as sediment centuries ago. The $\delta^{13}C$ and C/N decrease in buried in situ profiles had the same tendency as recent forest soil, indicating constant SOM quality distribution after burial. Accordingly, microbiological activity, root uptake, and metabolism have not been

effective enough to modify initial soil properties.

Keywords

$\delta^{13}C$
$\delta^{15}N$
Sedimentation
Soil erosion
Soil organic carbon

Responsible editor: Nikolaus Kuhn

1. Introduction

Soil erosion is one of the most effective soil transporting agents in recent surface evolution (Poesen 2015). Soil erosion in general, and especially sheet erosion, removes, delivers, and deposits uppermost soil layers which are usually relatively rich in organic matter (OM) (Lal et al. 2008; Szalai et al. 2016). Soil organic matter (SOM) quantity and composition reflects to the former soil formation processes and evolution conditions, including climate, land use, topography, and hydraulic conditions. Among others, soil loss and deposition processes can be estimated on the basis of the spatial distribution of SOM quality and quantity. However, additional estimation methods for soil redistribution and sedimentation are calculated using proxies such as soil texture (Jankauskas and Fullen 2002), soil organic carbon (SOC) content (Polyakov and Lal 2008; Wang et al. 2010; Farsang et al. 2012), or radionuclides (Mabit et al. 2008). Furthermore, SOM quality can provide additional important details on soil redistribution processes (Novara et al. 2015; Szalai et al. 2016). On the other hand, SOM cannot be accurately typified using average chemical composition, since it is a mixture of organic components at different stages of decomposition. For better characterization, certain physical and chemical properties are measured, such as solubility in various media (Kononova 1966), absorbance values of SOM solutions at different wavelengths (Tan 2003; Her et al. 2008), element ratios (Watteau et al. 2012), molecular sizes, weights and zeta potential (Esfahani et al. 2015), (diffuse) reflectance spectra (Viscarra Rossel et al. 2006; Conforti et al. 2013), and labiality (Zimmermann et al. 2007).

AQ2

A widespread method for SOM description is the measurement of carbon and

nitrogen isotope ratios within SOM. These data are generally used to assess soil system changes due to cultivation. Hence, there are major differences between the OM synthesized by C3 and C4 photosynthesis. Organic matter built by C4 plants has $\delta^{13}C$ value ~ − 12‰, while C3 plants produces ~ − 25‰ (Balesdent et al. 1987). Since the primary source of SOM is the dead biomass, changes in SOM, isotope ratios are the result of changes in vegetation patterns. Globally, almost 95% of plants belong to the C3 group, while C4 plants are mainly situated in the tropics. The most common C4 plant is maize, since it covers the highest proportion of arable lands in Hungary. Maize (corn) became essential grain in the seventeenth century in the whole country. At that time, most arable lands were occasionally sown with maize. From that time, the $\delta^{13}C$ value of the cultivated soils gradually increased, due to increasing C4 residuals.

In addition to OM inputs, the mechanisms and rates of SOM decay can determine or change $\delta^{13}C$ values in the soil via three main processes (Wynn et al. 2006). These are described below. (i) Kinetic fractionation occurs since heavy isotopes have a slower reaction rate that increases $\delta^{13}C$ concentrations. This general change follows a logarithmic function based on Rayleigh fractionation (Guillaume et al. 2015). Accordingly, during the SOM maturation processes, each abiotic environmental influence that decreases SOM mineralization (such as either lower temperature or precipitation amounts) can decrease $\delta^{13}C$ values (Austin and Vitousek 1998). (ii) During preferential substrate decomposition certain readily decomposable substances, such as amino acids and sugars, contain higher $\delta^{13}C$ concentrations, while more stable components such as lignin or lipids tend towards negative $\delta^{13}C$ signatures. (iii) Rapid growth of microbiological biomass can also increase the proportion of ^{13}C (Dijkstra et al. 2006); hence, it has significantly higher values compared to SOM (Werth and Kuzyakov 2010). Continuous SOM maturation by microbes can gradually increase $\delta^{13}C$ (Gunina and Kuzyakov 2014). On the other hand, mean $\delta^{13}C$ soil values could be a function of climatic parameters. Stevenson et al. (2005) found an inversely proportional relationship between mean annual precipitation and $\delta^{13}C$ ratios in soil. Bird et al. (2004) concluded the same tendency in Botswana along a 1000-km-long transect. Moreover, they found a direct connection between mean annual precipitation (MAP) and topsoil SOC content. This linkage disappears > 500 mm MAP. In undisturbed, natural soil profiles, the vertical distribution of SOM content and $\delta^{13}C$ values are inversely proportional (Novara et al. 2015).

The distribution of ^{15}N in soils follows rules both at landscape and profile

scales. However, generally on a global scale, values in soil vary between – 5 and + 12.6‰ (Craine et al. 2015). At the landscape scale, in the morphologically deeper positions where temporary water saturation can occur, the proportion of ^{15}N is generally higher due to increased denitrification activity (Mukundan et al. 2010). The same is true in a smaller scale within soil profiles concerning layers with low permeability or compact bedrock. The $\delta^{15}N$ values also could have a distinct vertical distribution within a soil/sediment profile, depending on differences in the sediment and decomposition rates. Therefore, they could be a useful tracer for sediment fingerprinting, especially for the identification of sediments eroded by gully or subsoil erosion (Laceby et al. 2015).

Changes of $\delta^{13}C$ and $\delta^{15}N$ values within in situ soil profiles (Schneckenberger and Kuzyakov 2007) or human-constructed terraces (Vázquez et al. 2015) are studied and interpreted as the results of past land uses. Some decrease could be due to major changes in global atmospheric ^{13}C, concentration due to the Industrial Revolution and the greater use of fossil fuels, widely known as the Suess effect (Suess 1955; Levin et al. 1989). Guillaume et al. (2015) found the stable isotope measuring method a powerful tool to estimate the degree of erosion from soil profiles which had experienced major land use changes (e.g., rainforest to arable land). Novara et al. (2015) investigated results on erosion and redistribution processes under vineyards using stable isotope techniques. However, little is known about the applicability of stable isotope ratios in studying soil redistribution processes (erosion and deposition) within arable fields.

Most studies have taken place in the tropics, because SOM mineralization and the exact change between C4 and C3 plants are most intense and common there (Nottingham et al. 2015). Moreover, in a global context, soil erosion mainly endangers tropical soils, while Mediterranean soils are usually already excessively eroded. Thus, the secondary spatial concentration of stable carbon isotope research on soil redistribution and degradation has focused on Mediterranean environments (Novara et al. 2014a, b, 2015; Vázquez et al. 2015) but relatively few studies have reported results from the temperate zone (Zhang et al. 2015; Zollinger et al. 2015).

Even though many papers are published on soil erosion each year, deficiencies remain in assessments of the degree and temporal dynamics of agriculture-accelerated surface development at the field scale (Poesen 2015). Therefore, the aims of this study were (i) to establish whether C and N stable isotope

patterns in deposited profiles are adequate proxies to identify the temporal distribution of surface development beyond the present and initial stages and (ii) to make numerical predictions on sedimentation volumes based on stable isotope distribution techniques.

2. Materials and methods

2.1. Study site

The study was conducted at Ceglédbercel (47.249221°, 19.678067°) on intensively cultivated arable land south east of Budapest central Hungary (Fig. 1). Previous investigations demonstrated that this field site was representative of local cropland and suitable for historical soil erosion studies (Jakab et al. 2016; Szalai et al. 2016). Moreover, landscapes with very similar properties and processes are widespread in Western and Central Europe, where soil erosion became serious due to forest clearance in historical times (Cerdan et al. 2010).

Fig. 1

Location of the Ceglédbercel study site. Dots indicate the boreholes involved in this study. Slope sections indicate the slope positions of the boreholes and solum depth. The contour line interval is 2.5 m

AQ3

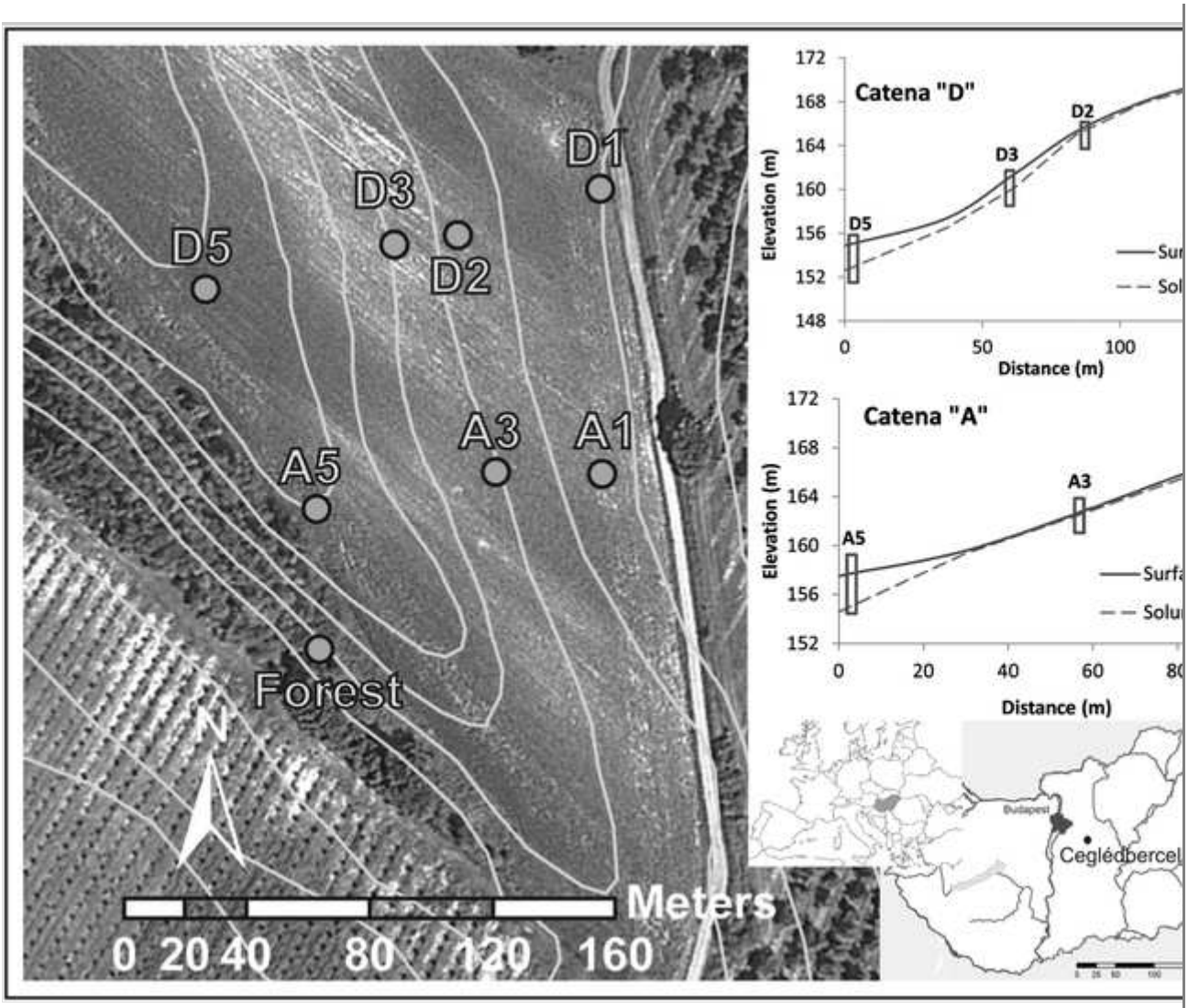

The catenas represent two convex-concave complex slopes with a narrow inflection strip in the middle. Soil was formed on a Quaternary sandy loess parent material, originally under forest vegetation. Land use change (forest to crop field) dates were calculated on the basis of local historical maps (Szalai et al. 2016). After forest clearance in the early eighteenth century, soil and tillage erosion developed and reformed the soil profiles along the slopes. Both sheet and tillage erosion were identified as the main driving processes, those diminished soil depth at the slope shoulder and deposited soil loss at the toe-slope, whereas no signs of linear erosion were observed (Fig. 1). The investigated catenas were individual erosion units without relevant external in- or outflow. Erosion rates were calculated by Szalai et al. (2016) for the field, with a maximum of 3 mm year^{-1} (loss of 1 m soil layer) at the most eroded spots, that resulted approximately 2 m sedimentation at the toe. Moreover, laboratory rainfall simulations identified sediment concentration values 6–50 g L^{-1} (Szabó et al. 2015) that also underlined the high vulnerability of the site against sheet erosion. Thus, soil types of the study

field have become heterogeneous, including Eutric Calcaric Cambisols, Loamic and Eutric Calcaric Ochric Regosols (IUSS WRB 2015) (Szalai et al. 2016). Cambisols and Regosols cover considerable parts of the temperate zone and are prone to soil erosion (Parras-Alcántara et al. 2015; Szabó et al. 2017). The main properties of the soil are in Table 1. Slope steepness of the current surface varies between 5 and 17% with a mean of 12%, on elevations between 154 and 170 m a.s.l. Mean annual precipitation is ~ 600 mm, while mean annual temperature is 10.8 °C (Dövényi 2010). The investigated section has been cultivated in the slope direction using conventional tillage techniques. Since forest clearance, the appearance of C4 plants (maize) was occasional, but C3 crops (e.g., winter wheat, sunflower, and rape) still remained predominant. The tilled layer of this field was also investigated using rainfall simulation experiments, in order to measure initial SOC and SOM erosion in the sub-meter scale (Jakab et al. 2016).

Table 1

The main properties of the investigated soil (composite sample from the cultivated layer) (after Jakab et al. 2016)

AQ4

Property		**SD**	**1:10 extract in distilled water**		
Color	10YR 3/3		Conductivity	$\mu S\ cm^{-1}$	137.0
pH (distilled water)	7.63		pH		8.2
pH_{KCl}	7.13		Alkalinity	$cmol_+\ L^{-1}$	8.1
CEC ($cmol_+\ kg^{-1}$)	11.08	0.09	HCO_3^-	$mg\ L^{-1}$	46.7
Al_2O_3 ($m\ m^{-1}$)	12.15	0.04	Total hardness	$cmol_+\ L^{-1}$	11.2
MnO ($m\ m^{-1}$)	0.11	0.01	Ca^{2+}	$mg\ L^{-1}$	22.9
MgO ($m\ m^{-1}$)	1.89	0.04	Mg^{2+}	$mg\ L^{-1}$	0.0
CaO ($m\ m^{-1}$)	5.23	0.04	Permanent hardness	$cmol_+\ L^{-1}$	4.0
SiO_2 ($m\ m^{-1}$)	57.22	0.51	Cl^-	$mg\ L^{-1}$	0.0
P_2O_5 ($m\ m^{-1}$)	0.33	0.00	NO_3^-	$mg\ L^{-1}$	44.63
TiO_2 ($m\ m^{-1}$)	0.66	0.01	SO_4^{2-}	$mg\ L^{-1}$	13.7
Fe_2O_3 ($m\ m^{-1}$)	3.92	0.03	K^+	$mg\ L^{-1}$	1.16
K_2O ($m\ m^{-1}$)	2.54	0.02	Na^+	$mg\ L^{-1}$	0.57
SD standard deviation, *CEC* cation exchange capacity					

2.2. Sampling

Soil sampling was conducted in summer 2013 as a part of a holistic sampling campaign, in which 100 soil samples were removed from 47 boreholes using hand auger. These samples were gathered from representative layers of the solum with varying thickness. Detailed description of the sampling process is reported in Szalai et al. (2016). In the present study, only 33 samples are investigated and discussed, including four soil profiles, and four additional samples from the uppermost tilled layer from the Regosol points (Fig. 1). The profiles/samples represent in situ soils at the (i) inflection strip (D3); (ii) eroded parts (A1, A3, D1, D2); (iii) depositional surfaces (A5, D5); and (iv) intact profile under forest (presumed to be non-eroded and without severe sedimentation) (Jakab and Kertész 2014) (Fig. 1). In coding letters stand for the parallel catenas and numbers indicate slope position (1—up-slope; 3—mid-slope; 5—toe-slope).

2.3. Chemical analysis

To quantify relationships between particle size and stable isotope distribution, soil texture was determined. For particle size analysis, the samples were treated with 0.5 M sodium pyrophosphate ($Na_4P_2O_7 \times 10H_2O$) and 15 min ultrasonic agitation in order to breakdown aggregates. Particle size distribution was measured using a laser diffraction particle sizer (Horiba Partica LA-950) within a range of 0.2–2000 μm (Centeri et al. 2015). The particle size calculating method was based on Mie theory (Mie 1908). For compatibility with pipette method 8 μm was used as the upper diameter value for the clay fraction (Konert and Vandenberghe 1997). Inorganic carbon content was measured using the gas volumetric method of Scheibler (Pansu and Gautheyrou 2006). For SOC and $\delta^{13}C$ investigations, the inorganic carbon was removed from samples using 19% HCl. Acid treatments were repeated until the completion of CO_2 release. Nitrogen and SOC content was measured using an element analyzer (Tekmar Dohrman Apollo 9000N) (Buurman et al. 1996). Carbon/nitrogen ratio was calculated on the basis of the result of elemental analysis. Stable carbon and nitrogen isotope signatures were measured using a Thermo Scientific FLASH 2000 HT Elemental Analyzer mass spectrometer. Polyethylene [(CH_2)n] and urea calibrated to IAEA standards were used as references. Samples were measured in triplicate. Where standard deviations were > 10% repeated measurements were used.

Stable carbon isotope composition is expressed as the ratio of ^{13}C isotopes to

^{12}C ($\delta^{13}C$) in parts per thousand (‰). Since most of the values in nature are too small in this scale, zero value was set to a standard of a marine fossil (Belemnitella americana), which has an extremely high and uniform ratio of 0.0112 as a convention. This fossil was from the Pee Dee formation hence was called Pee Dee Belemnite (V-PDB). Therefore, ‰ values used in soil science and also in this study are related to V-PDB as zero, which triggered negative values.

Similarly, stable nitrogen isotope composition is expressed as the ratio of ^{15}N and ^{14}N in parts per thousand (‰). In nature, approximately 0.36% nitrogen is in ^{14}N form. For standard, atmospheric molecular nitrogen (AIR) is used which by convention is set to 0‰. This way, studied SOM samples were compared to standards according to Eq. (1):

$$\delta = \left(\frac{R_{\text{sample}}}{R_{\text{standard}}} - 1 \right) * 1000 \qquad 1$$

where R is the $^{13}C/^{12}C$ ($^{15}N/^{14}N$) ratio in the sample or in the international standard (Coplen 2011).

Molecular properties of SOM were estimated on the basis of photometric properties using absorbance spectra of alkali solved SOM. Sodium hydroxide (NaOH) solution (0.5 M) was applied for SOM extraction from soil. Extracted SOM were characterized by recording their absorbance spectra in a wavelength range of 1800–180 nm. Absorbance values at distinct wavelengths were used to calculate indexes, such as E_4/E_6 and E_2/E_3 indexes as proxies of the degree of mean polymerization (Tan 2003) as well as ultraviolet absorbance ratio index (URI, UVA_{210}/UVA_{254}) as an indicator for mean functional group density (Her et al. 2008) of SOM. Absorbance value at 280 nm was applied to estimate the mean degree of aromaticity (Chin et al. 1994) of SOM molecules.

3. Results and discussion

Solum depth varied 0–280 cm in the studied profiles. In the eroded parts, the recent solum was formed due to cultivation therefore its depth ≤ 25 cm. The in situ site under the forest was 110 cm deep, while the profile in the inflection (D3) was 100 cm. The measured properties of each catena are reported in Table 2.

Table 2

Measured properties of the soil samples on the Ceglédbercel catena

Profile	Depth (cm)	dN (‰)	dC (‰)	Clay[a] (%)	Silt[b] (%)	Sand[c] (%)	URI	E_4/E_6	280 Abs.	E_2/E_3
A1	0–10	4.1	−23.0	32.7	23.2	44.17	1.48	3.00	1.53	2.80
A3	0–10	5.3	−23.7	26.2	21.9	51.82	1.09	3.13	1.58	2.76
A5	0–25	5.9	−24.9	33.3	24.3	42.40	1.00	2.65	2.11	2.47
A5	25–50	7.1	−25.4	31.0	25.2	43.77	1.36	3.22	1.75	2.71
A5	50–80	7.7	−25.5	36.3	28.5	35.23	1.41	3.53	1.24	2.84
A5	80–110	7.2	−25.6	29.7	27.3	42.99	1.46	5.93	1.20	2.95
A5	110–140	6.8	−25.7	31.4	28.0	40.65	1.37	4.42	1.12	2.82
A5	140–160	6.5	−25.7	32.5	29.3	38.19	1.47	6.70	0.95	2.87
A5	160–185	5.8	−25.6	27.8	24.6	47.53	1.62	4.73	0.85	2.78
A5	185–210	5.3	−25.4	28.7	27.8	43.53	2.08	4.71	0.50	3.04
A5	210–250	5.5	−25.2	29.2	26.4	44.38	1.81	3.04	0.49	2.81
A5	250–280	5.7	−25.3	31.2	28.0	40.76	2.35	3.27	0.35	3.08
D1	0–10	5.3	−24.2	38.3	23.5	38.22	1.59	13.20	1.21	3.26

dN and dC stand for stable isotope ratios. E_2/E_3 and E_4/E_6 are indexes as parameters matter polymerization (Tan 2003)

URI ultraviolet absorbance ratio index (ratio of absorbance values measured at 210 ar *280 Abs*. measured absorbance at 280 nm as a proxy of aromaticity, *SOC* soil organic carbon/nitrogen ratio

[a] < 8 μm measured by laser diffraction

[b] 8 μm–50 mμ Please change the order.

[c] > 50 μm

Profile	Depth (cm)	dN (‰)	dC (‰)	Clay[a] (%)	Silt[b] (%)	Sand[c] (%)	URI	E_4/E_6	280 Abs.	E_2/E_3
D3	0–10	6.3	−24.5	33.5	24.6	41.83	1.71	2.24	0.94	2.81
D3	50–60	6.4	−24.8	38.9	26.6	34.55	1.96	2.88	0.68	3.25
D3	80–90	6.8	−24.7	42.3	26.7	31.00	2.12	n.a.	0.52	3.78
D4	0–10	3.6	−22.9	26.0	24.7	49.34	2.16	1.97	0.72	2.79
D5	0–30	5.7	−24.5	29.2	23.3	47.56	1.44	2.34	1.31	2.98
D5	30–80	6.9	−25.1	36.4	24.4	39.25	1.59	3.90	1.12	3.17
D5	80–110	7.2	−25.6	42.7	28.5	28.86	1.47	2.46	1.32	2.91
D5	110–125	7.1	−25.6	41.4	30.4	28.13	1.56	3.71	1.09	2.97
D5	150–160	6.3	−25.6	39.4	26.2	34.38	1.75	2.26	0.94	2.79
D5	180–190	4.7	−25.6	32.1	25.1	42.79	1.93	2.70	0.76	2.73
D5	200–210	5.8	−25.6	30.7	25.5	43.81	2.17	1.74	0.62	2.60
D5	210–220	4.9	−25.4	34.9	27.5	37.64	2.83	2.61	0.29	3.21
Forest	0–24	5.0	−25.4	36.1	23.2	40.68	1.93	3.00	2.53	2.95
Forest	30–45	6.1	−25.3	37.5	26.7	35.83	2.64	2.76	1.84	2.95

dN and dC stand for stable isotope ratios. E_2/E_3 and E_4/E_6 are indexes as parameters matter polymerization (Tan 2003)

URI ultraviolet absorbance ratio index (ratio of absorbance values measured at 210 ar *Abs*. measured absorbance at 280 nm as a proxy of aromaticity, *SOC* soil organic carb carbon/nitrogen ratio

[a]< 8 μm measured by laser diffraction

[b]8 μm–50 mμ Please change the order.

[c]> 50 μm

Profile	Depth (cm)	dN (‰)	dC (‰)	Clay[a] (%)	Silt[b] (%)	Sand[c] (%)	URI	E_4/E_6	280 Abs.	E_2/E_3
Forest	45–54	6.9	−25.3	34.4	25.0	40.63	3.89	2.26	1.23	2.96
Forest	70–80	6.2	−25.1	32.4	26.3	41.32	4.92	1.90	1.00	2.44
Forest	95–102	6.4	−25.1	32.4	24.5	43.08	6.01	1.77	0.83	2.50
Forest	106–110	3.4	−25.2	38.2	26.9	34.90	7.83	1.65	0.61	3.00

dN and dC stand for stable isotope ratios. E_2/E_3 and E_4/E_6 are indexes as parameters matter polymerization (Tan 2003)

URI ultraviolet absorbance ratio index (ratio of absorbance values measured at 210 ar *Abs*. measured absorbance at 280 nm as a proxy of aromaticity, *SOC* soil organic carb carbon/nitrogen ratio

[a]< 8 μm measured by laser diffraction

[b]8 μm–50 mμ Please change the order.

[c]> 50 μm

3.1. Spatial distribution of SOC

Distribution of SOC content varies with depth in the investigated profiles (Fig. 2). Profile D3 and the forest profile have a pattern of gradually decreasing SOC with depth, which is considered representative of the natural vertical distribution. The content and the trend of decreasing SOC below 50 cm are quite similar, but the SOC content of the uppermost 50 cm differs. Over 10 g kg^{-1} SOC is absent in the tilled layer of profile D3. This could be the result of (i) SOC mineralization of SOC due to intensive cultivation or (ii) soil erosion and/or deposition in the D3 profile. On the other hand, surface sample properties are highly variable and measured values seem to be independent from morphological position. Many studies report data on SOC enrichment down-slope (Wang et al. 2010; Farsang et al. 2012). Szalai et al. (2016) found SOC deposition spots on the toe-slope of the same research site. This suggests that beyond mass movement spatial heterogeneity of selective SOM deposition or mineralization may hardly affect local SOC contents. Thus, soil surface properties are highly variable even under intensive cultivation.

Fig. 2

Changes in SOC content of the studied profiles. Shallow profiles, such as A1; A3 and D1; D4 are included in “surface samples” (error bars indicate standard deviation), *n* = 3–6 (depending on standard deviation)

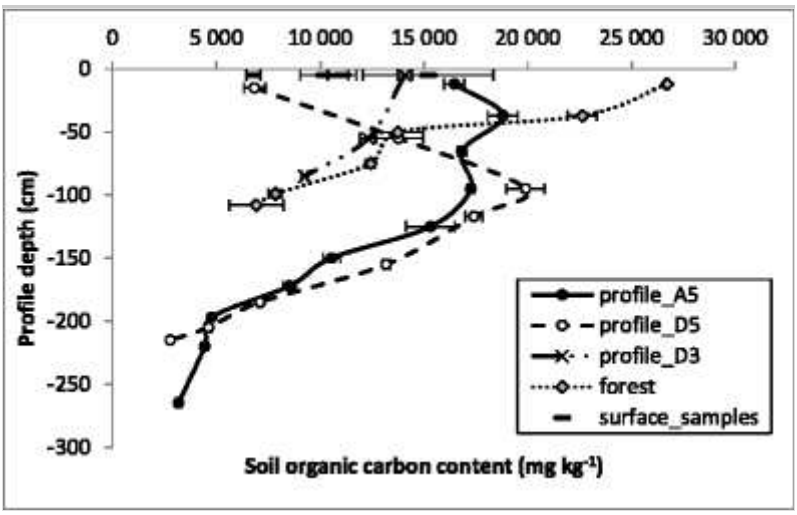

In contrast, SOC content in profiles A5 and D5 reach their maximum value below the surface at depths that relate to sedimentation in these parts of the landscape (Fig. 2). Profile A5 has a bimodal distribution due to periodical changes in the SOC concentrations of sediments, while in profile D5 there is a definite peak at ~ 1 m depth.

3.2. Spatial distribution of $\delta^{13}C$

Besides the high variance in SOC content of the uppermost cultivated layer samples of each crop field profile, they have higher $\delta^{13}C$ values, with very high variance (Fig. 3). This could be the result of the more frequent sowing of maize in recent decades. High variance refers to the altering decomposition degrees of the relatively recent plant residuals. An additional possibility is selective decomposition. However, Vázquez et al. (2015) stated that decreased tillage intensity results in higher C/N ratios and the increase of $\delta^{13}C$ values and vice versa.

Fig. 3

Changes in $\delta^{13}C$ values in the investigated profiles (error bars indicate standard deviation) *n* = 3–6 (depending on standard deviation)

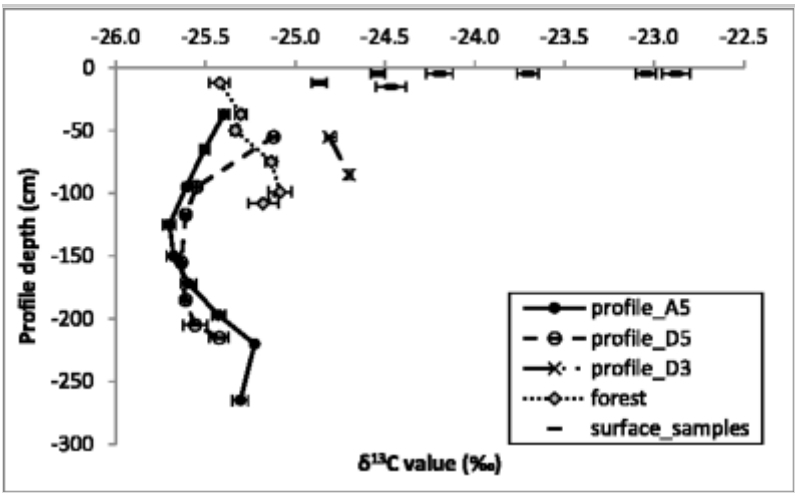

According to the results of Stevenson et al. (2005), pedogenic carbonates have significantly higher $\delta^{13}C$ values within a range of − 4.1 to − 10.8‰ that ensure the possibility of separation of organic and inorganic carbon solely on the basis of stable isotope concentrations. Accordingly, the higher values could be the result of $CaCO_3$ exhumed from the parent material due to intensive erosion. However, the samples in question were completely decarbonated by HCl. It is postulated that some of the most reactive SOM components, such as sugars and proteins, could be mobilized by the acid application and leached out during the acid removal process. Since all samples were treated the same way, this is probably not the reason for the higher values in the cultivated layer.

Soil samples beneath the tilled layer had a significantly lower ^{13}C values with much less variation (Fig. 3). The range is between − 24.5 and − 25.8‰, which completely covers the C3 plant residuals (Balesdent et al. 1987). This suggests that the main part of soil redistribution on the investigated field occurred prior to the widespread farming of maize in the eighteenth century in Hungary (Hadi 2006). According to this scenario, the main erosion and redistribution processes occurred immediately after forest clearance (Vanwalleghem et al. 2006), but before the frequent growth of maize (first half of the eighteenth century).

Only profile D3 had higher signature values, those are still less than surface samples. Since this profile is on the inflection section, on the basis of its depth and vertical SOC distribution, it could be original and intact. On the other hand, because of the long time elapsed since forest clearance on the site, this profile could be completely eroded and redeposited again. This variation, however, shows a consequent spatial distribution. On the sedimentary parts,

soil profiles have a specific U-shaped $\delta^{13}C$ value distribution with depth (Fig. 3).

The smallest $\delta^{13}C$ value is ~ 130–150 cm depth, which is presumed to be the original soil surface prior to the onset of accelerated erosion processes. This does not accord with the SOC content distribution since SOC has a maximum higher in the profile, at 100 cm depth. This difference of 30 cm suggests that immediately after forest clearance when erosion rates accelerated, selective erosion (Lal and Pimentel 2008 Lal et al. 2008) caused SOC enrichment of sediment. Thus, deposited soil loss with a higher SOC content covered the lower parts of the catena (A5 and D5 profiles). After the deposition of this ~ half a meter of sediment, the SOC content of soil loss became lower because of the loss of SOM enriched “A” horizons on the upper parts of the catena. Hence, erosion mobilized and delivered much less SOC, which presumably created the upper part of the sedimentary profiles.

AQ5

The original, buried soil profiles have increasing $\delta^{13}C$ values with depth, which accords with the results of Novara et al. (2014a, b, 2015). Vázquez et al. (2015) also found that values of $\delta^{13}C$ increased with depth in all pedons and decreased from the top to the bottom of the slope. Catena A followed this trend and there was a distinct decrease in $\delta^{13}C$ values along the slope in the tilled layer, while in catena D, there was no apparent connection among SOC content, $\delta^{13}C$ values and geomorphologic position (Table 2).

Wynn et al. (2006) reported logarithmic increases of $\delta^{13}C$ in both cultivated and control soil profiles. The trend observed in this study is probably linear rather than logarithmic (Fig. 4). This increasing value is most likely explained by the greater degree of decomposition in deeper horizons resulting from SOM maturation with depth (Wynn et al. 2006). Quite similar tendencies were observed in the neighboring profile in the forest (Fig. 4), which is the natural undisturbed vertical distribution. Wynn et al. (2006) found that $\delta^{13}C$ distribution was not clearly logarithmic in the cultivated profiles, but has a shift to 1‰ upwards compared to the control site. In the control site, the distribution could be described using the Rayleigh distillation model. However, in that case the range of $\delta^{13}C$ varied within a wide range between − 22 and − 28‰. As the shape of the fitted lines are quite similar in the buried and forest profiles, there was no significant SOM maturation since burial in the present case. Consequently, burial conserved the vertical distribution of

$\delta^{13}C$; therefore, no detectable maturation or SOM decomposition occurred. In profile D3, $\delta^{13}C$ decreased with depth (Fig. 3). Compared to the regular vertical SOC distribution, this profile seemed to be similar, therefore in situ.

Fig. 4

Changing $\delta^{13}C$ values in the in situ parts of the profiles follow a linear function (error bars indicate standard deviation) $n = 3–6$ (depending on standard deviation). n.s., not significant

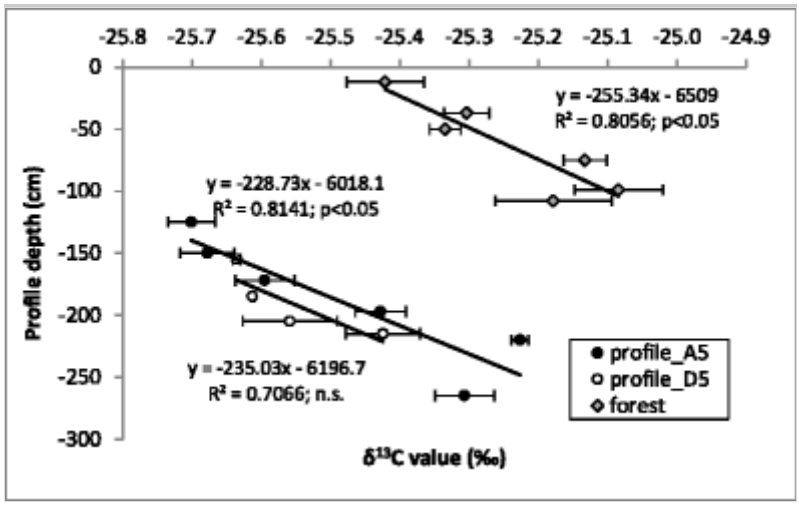

The steepness of the fitted linear functions was one order of magnitude higher in Mediterranean vineyards (Novara et al. 2015), which supported the existence of linear connection also found in this study, nevertheless emphasized the role of local modifying (probable mineralization related) parameters. However, this model has ambiguities, since it does not take into account selective erosion and deposition and carbon sequestration and mineralization (Fiener et al. 2015; Doetterl et al. 2016; Hu and Kuhn 2016).

As in this study (Table 2), Laceby et al. (2015) also found no correlation between particle size distribution and $\delta^{13}C$ or $\delta^{15}N$ values. However, Bellanger et al. (2004) reported associations between specific size fractions with different $\delta^{13}C$ concentrations. The reason of this contradiction may be the different age of SOM attached to soil particles. This can result in various $\delta^{13}C$ values due to land use and/or agrotechnical changes. According to Bai et al. (2012), the (measured) $\delta^{13}C$ values can also be a function of soil texture. They found a positive significant correlation between silt + clay fraction and $\delta^{13}C$ value. Moreover, according to their results, SOC concentration is significantly and negatively correlated with $\delta^{13}C$ values. They concluded that SOC is mostly derived from roots rather than shoot derived (above ground)

plant residuals. Metabolites of C4-type photosynthesis persist longer in organo-mineral complexes and thus increase $\delta^{13}C$ values compared to sandy soils deficient in fine-sized particles. The depositional, upper parts of the A5 and D5 profiles have an opposite distribution in which δC^{13} values decrease with depth (Fig. 3). Since the cultivated surface layer has significantly lower values, their deposition on toe-slopes is a plausible explanation. In the original undisturbed parts (beneath the deposition layers), $\delta^{13}C$ values appear to be largely a function of SOC content (Fig. 5). There is a reciprocally proportional linear linkage between them; however, the steepness of the fitted trend lines varies. In the cultivated eroded and deposited parts there is no significant correlation, which accords with Vázquez et al. (2015), who reported $\delta^{13}C$ variations to be independent from the C content along the depth of a manmade terrace in Spain since terrace soils were typically mixed.

Fig. 5

Connection between SOC and $\delta^{13}C$ values in the in situ parts of the investigated profiles (error bars indicate standard deviation) $n = 3–6$ (depending on standard deviation). n.s., not significant

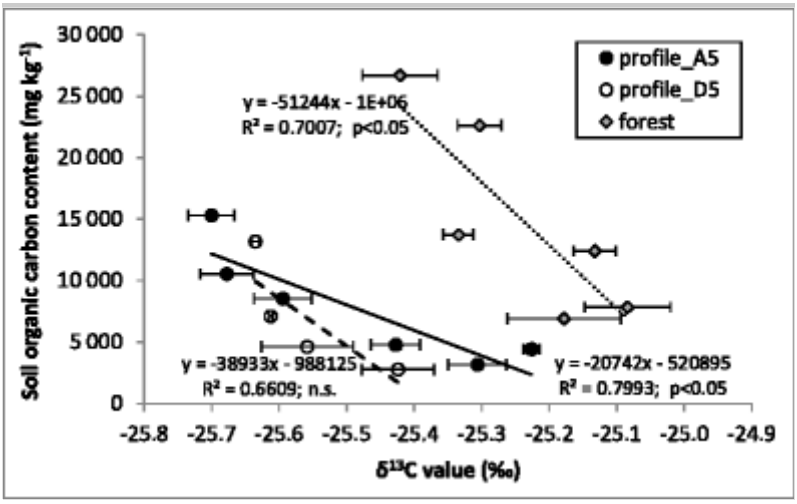

The higher the SOC content, the lower the $\delta^{13}C$ value, which was interpreted by Austin and Vitousek (1998) as the higher resistance of the heavier molecular weight carbon that finally resulted in $\delta^{13}C$ enrichment in the mineralized parts. On the basis of the results presented above, the burial of these profiles occurred over 200 years ago that limited SOM decomposition processes in these layers, and accordingly selective decomposition was less effective (Van Oost et al. 2007). This relationship is assumed to have developed during SOM formation, as was the case in the forest profile. According to this theory, the most mobile components had higher $\delta^{13}C$ values

that could increase this in deeper horizons, due to the higher ratio in migrating SOM.

3.3. Spatial distribution of N and C/N

Generally, SOM quality tends to be fairly constant within a small scale, homogenous land use unit, which suggests a narrow range of C/N ratio within this homogeneous unit. In contrast, in the present study, the spatial distribution of the TN content compared to that of the carbon shows a different pattern (Fig. 6).

Fig. 6

Plot of soil nitrogen values (**a**) and C/N ratios (**b**) with depth (in the investigated profiles (error bars indicate standard deviation) $n = 3–6$ (depending on standard deviation)

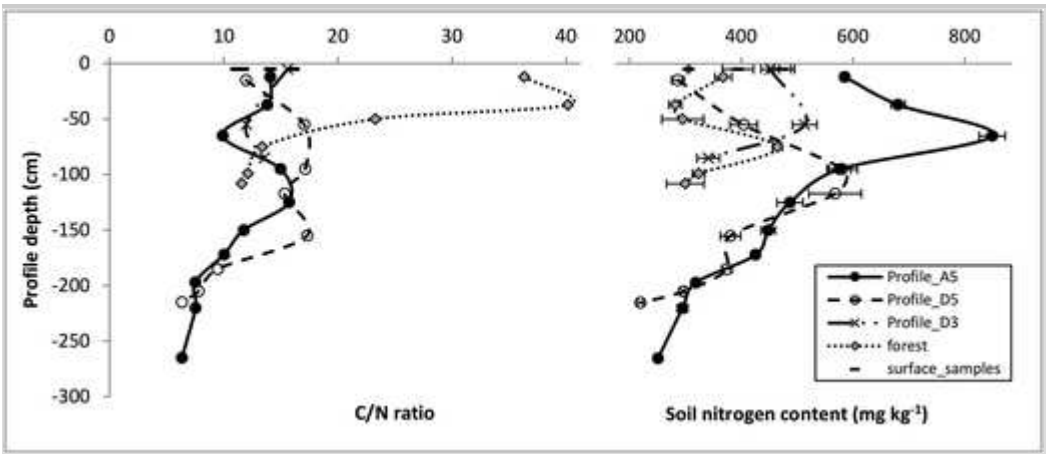

The highest difference is found in the case of the forest profile, especially in the upper part. Here, a relatively high SOC content, paired with a relatively low TN concentration, results in a C/N ratio of ~ 40. This implies the dominance of the forest derived, weakly decomposed SOM.

The most salient point indicated by the TN peaks is in the depth range of 0.5–1.2 m depth, while the value on the surface is much lower in each cultivated profile. This suggests increased selective SOM decomposition in the upper layers, probably due to intense physical disturbance (aggregate breakdown) and greater oxidation (Kuhn et al. 2012). The undisturbed forest profile had the same vertical pattern that could not be affected by tillage. In profiles A5 and D5, these TN peaks could refer to the original soil surface, as it does with SOC patterns. However, SOC peaks and $\delta^{13}C$ abundance

indicated the original surface at a lower level of 1–1.5 m. In soils, environmental conditions (e.g., moisture, temperature, available and biologically active N and pH) can limit SOM decomposition and maturation processes. Therefore, its concentration can change much more rapidly as a function of temporal variations in biological activity (Liang et al. 1999).

In each in situ soil profile (forest and the lower parts of A5 and D5), C/N ratios show a decreasing trend with depth, while in the sedimentary sections there are no clear trends. Taking the decreasing curves as a proxy of the original soil profile, the same deposition depth (~ 130 cm) is identified as calculated from the vertical pattern of $\delta^{13}C$.

3.4. Spatial distribution of $\delta^{15}N$

Recent N stock and forms in soil is believed to be the result of microbiologically driven complex progression. Thus, most studies on $\delta^{15}N$ focused on processes within the uppermost 10 cm of soil (Wang et al. 2014; Snider et al. 2017). Depth-related distributions were studied only in the upper 30 cm by Kerley and Jarvis (1997). However, they described TN increase and $\delta^{15}N$ decrease in an undisturbed soil profile with depth. In this study, $\delta^{15}N$ did not have a clear holistic spatial distribution, although there is a definite increase with depth in the uppermost 0.5–1.0 m layer. This ~ 1.0 m depth could be the limiting factor for biological activity. Boddey et al. (2000) also described irregular ^{15}N patterns with depth, even within in situ soil profiles. Generally, it is also true that the highest ^{15}N values in each profile in the present study were found at 0.5–1.0 m depth (Fig. 7), as in the case of the TN content (Fig. 6), which accords with the depth limit of microbiological activity discussed above.

Fig. 7

Plot of $\delta^{15}N$ values and depth in the investigated profiles (error bars indicate standard deviation) $n = 3–6$ (depending on standard deviation)

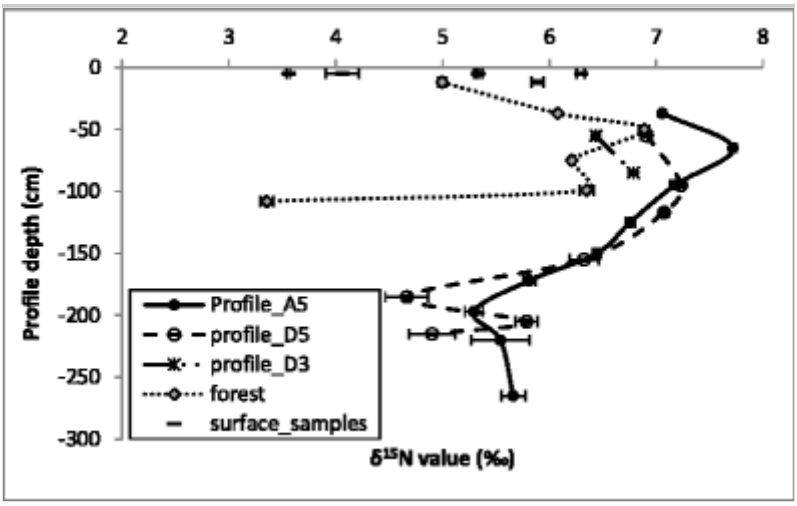

The $\delta^{15}N$ peak refers to the most mature SOM to be found in the 0.5–1.0 m layer, since during decomposition processes the ratio of the heavier fraction (^{15}N) increases in residuals in tandem with a decreasing C/N ratio (De Clercq et al. 2015), while the biologically active substrates are taken by plant roots. There could be a lack of mineralized N depleted in ^{15}N in this layer compared to the upper, and especially the surface layer, where microbial activity is generally of higher magnitudes. Therefore, most biologically active N forms remain in the layer, mainly within cells. Below this peak, both N content and $\delta^{15}N$ decrease with depth, as reported by Craine et al. (2015). The relatively lower values of the upper layers are the results of (i) high C/N ratios of the aboveground plant residuals; (ii) low SOM content, due to intensive cultivation; and (iii) low microbiological activity. Therefore, N distribution patterns are much more a function of microbial activity and hydrological conditions than SOC and $\delta^{13}C$ distribution, since they could vary seasonally ≤ 2.5‰ (Kerley and Jarvis 1999). Accordingly, N is much less suitable for retrospective surface identification predictions (Handley and Raven 1992).

While SOC content was linked with $\delta^{13}C$ only in the undisturbed in situ parts, there is a slight connection between TN content and $\delta^{15}N$ in the whole depth of both sedimentation profiles (A5, D5). Higher N content indicates higher $\delta^{15}N$ value, although in the forest profile and surface samples there is no significant correlation (Fig. 8). Accordingly, N amount determines the degree of maturation only in buried in situ profiles.

Fig. 8

Soil nitrogen content as a function of $\delta^{15}N$ (error bars indicate standard deviation) n = 3–6 (depending on standard deviation)

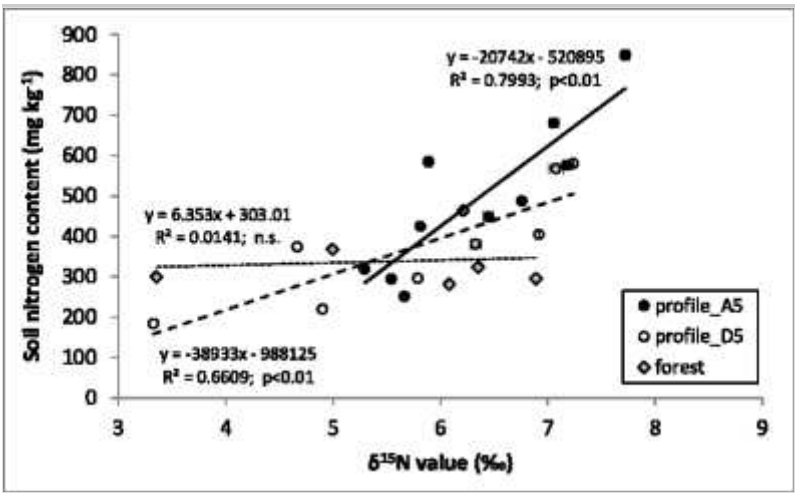

Former fertilization processes may have been influential. Manure and other animal wastes have higher $\delta^{15}N$ values (10–20‰), while SOM derived inorganic nitrogen (IN) has a range of 2–8‰ and artificial N fertilizers have the lowest range of – 2–3‰ (Freyer and Aly 1974; Kreitler et al. 1978). However, little is known about the isotopic fractionation processes of mineral N forms especially in the soils of the temperate zone (Boddey et al. 2000). Since little fertilizer or manure application has occurred in the study area, the lack of trends in the deposited and tilled soil layers could be the result of the occasional nutrient application.

Tiessen et al. (1984) found that 90 years of intensive tillage on a virgin prairie decrease the TN value by 51% but had little decrease effect on $\delta^{15}N$ in the bulk soil. On the other hand, ^{15}N abundance of most fractions could vary considerably. Inorganic nitrogen mineralized from SOM had lower values and extractable SOM had higher values, while the bulk soil as a whole remained constant (Koba et al. 2010). Others reported that dissolution of SOM components did not fractionate the isotopes (Amundson et al. 2003).

3.5. Connection between stable isotopes and soil properties

Many researchers found considerably stable connections between C and N stable isotopes in soil samples. In the present study, no relationship was found for the whole group of samples (Fig. 9). Although excluding the buried in situ and forest samples, a strong inverse correlation was found in eroded and deposited cultivated soil samples. Dijkstra et al. (2006) found this relationship to be inverse, both in the cases of total SOM and microbiological biomass. This relates to the parallel enrichment of stable isotopes during transformation and maturation processes. Thus, arable land acts as a separate

unit with a wider variation in both isotope ranges, while the in situ profiles seemed to be more stable and with less variability. This inverse linkage appears only in the cultivated and therefore strongly oxidized parts, suggesting differential transformation processes of C and N, namely selective isotope mineralization of C parallel with relatively stable δ^{15}N values.

Fig. 9

Relationships between the stable isotope values of soil samples

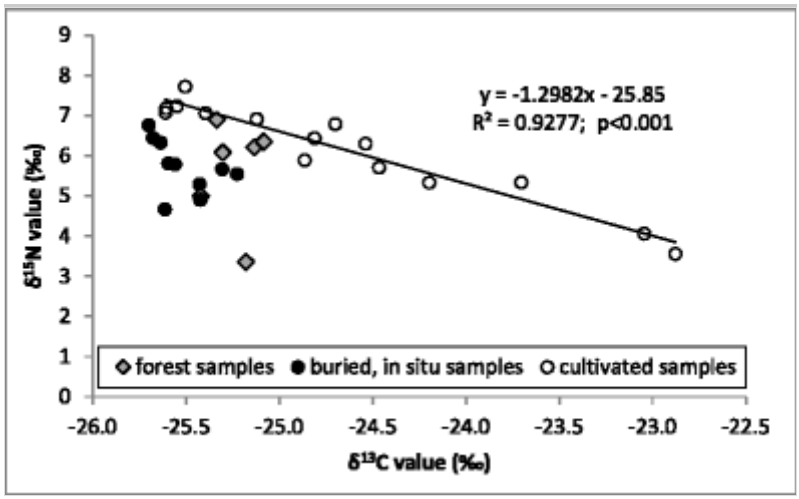

Although photometric and C/N ratio-based SOM properties varied in a wide range within the investigated site, there were no significant correlations between them and the stable isotopes (Table 2). This accords with the results of Yu et al. (2010) who reported considerable changes between δ^{13}C value of soil samples with various sources but found no significant difference in C/N values. Stable isotope ratios are properties of the in situ bulk SOM; however, photometric indexes are based on only the alkali soluble components of SOM, and accordingly, the soluble part does not represent the solid SOM as it was reported by Lehmann and Kleber (2015). However, C/N values also represent the bulk solid SOM the lack of connection suggests that stable isotope ratios of SOM components are independent from the degree of aromaticity or polymerization. Liang et al. (1999) published results on specific SOM component adsorption to various textured soils, but in the present case, no linkage was found between stable isotope values and soil texture. The absence of associations between particle size distribution and stable isotope ratios was presumed to be due to the lack of isotope selective bonds between organic and mineral components. Nevertheless, this study was based on a local soil type and SOM composition, in small scale; therefore spatial validity of absence of connection among SOM properties are limited.

4. Conclusions

The $\delta^{13}C$ and C/N decrease in buried in situ profiles had the same tendency as recent forest soil, indicating of the conservation of SOM quality distribution after burial. Accordingly, microbiological activity and root uptake and metabolism have not been effective enough to modify initial soil properties. These were in line with the results gained from the Mediterranean, even though the role of local modifying parameters was clear.

The highest SOC and TN values did not refer to the original buried soil surface, but rather with a layer of sediment deposited by selective initial erosion. On the other hand, $\delta^{13}C$ and C/N ratios indicated the original surface adequately to be ~ 1 m above parent material. This accords with the depth of the in situ forest profile and, if homogeneous soil depth is assumed, it means 70–80 cm soil loss from upper slopes. Consequently, at initial stages of sheet erosion, changes in $\delta^{13}C$ abundance due to tillage and delivery would much better fingerprint the original surface under sedimentation than SOC content.

Concentration of SOC and ^{13}C abundance within soil profiles are much more persistent than those of N. Therefore, the former are more suitable for estimating soil redistribution. More precisely, $\delta^{13}C$ patterns indicate the original soil surface, even in profiles sedimented centuries ago.

Most sedimentation occurred soon after forest clearance and before the start of intensive cultivation. This highlights the role of relief in sheet erosion intensity, compared to that of intensive tillage, which accords with the results of Szalai et al. (2016) at the same site.

Acknowledgements

The corresponding author was supported by the Bolyai János Fellowship of the Hungarian Academy of Sciences. The study was supported by OTKA K-100180. The authors are also grateful to E. Mészáros for SOC measurements and to the anonymous reviewers for their comments and suggestions.

References

Please remove the reference "Vitotello et al." from the list.

AQ6

Amundson R, Austin AT, Schuur EAG, Yoo K, Matzek V, Kendall C,

Uebersax A, Brenner D, Baisden WT (2003) Global patterns of the isotopic composition of soil and plant nitrogen. Glob Biogeochem Cycles 17:1031

Austin AT, Vitousek PM (1998) Nutrient dynamics on a precipitation gradient in Hawaii. Oecologia 113(4):519–529. https://doi.org/10.1007/s004420050405

Bai E, Boutton TV, Liu F, XB W, Hallmark CT, Archer SR (2012) Spatial variation of soil δ13C and its relation to carbon input and soil texture in a subtropical lowland woodland. Soil Biol Biochem 4:102–112

Balesdent J, Mariotti A, Guillet B (1987) Natural 13C abundance as a tracer for studies of soil organic matter dynamics. Soil Biol Biochem 19(1):25–30. https://doi.org/10.1016/0038-0717(87)90120-9

Bellanger B, Huon S, Velasquez F, Valles V, Girardin C, Mariotti A (2004) Monitoring soil organic carbon erosion with $\delta^{13}C$ and $\delta^{15}N$ on experimental field plots in the Venezuelan Andes. Catena 58(2):125–150. https://doi.org/10.1016/j.catena.2004.03.002

Bird MI, Veenendaal EM, Lloyd JJ (2004) Soil carbon inventories and δ13C along a moisture gradient in Botswana. Glob Chang Biol 13(3):342–349

Boddey RM, Peoples MB, Palmer B, Dart PJ (2000) Use of the ^{15}N natural abundance technique to quantify biological nitrogen fixation by woody perennials. Nutr Cycl Agroecosyst 57(3):235–270. https://doi.org/10.1023/A:1009890514844

Buurman P, van Lagen B, Velthorst EJ (eds) (1996) Manual for soil and water analysis. Backhuys Publishers, Leiden

Centeri, Cs, Jakab G, Szabó SZ, Farsang A,·Barta K,·Szalai Z, Bíró ZS (2015) Comparison of particle-size analyzing laboratory methods. Environ Eng Manag J 14(5):1125–1135

Cerdan O, Govers G, Le Bissonnais Y, Van Oost K, Poesen J, Saby N, Gobin A, Vacca A, Quinton J, Auerswald K, Klik A, Kwaad FJPM, Raclot D, Ionita I, Rejman J, Rousseva S, Muxart T, Roxo MJ, Dostal T (2010)

Rates and spatial variations of soil erosion in Europe: a study based on erosion plot data. Geomorphology 122(1–2):167–177. https://doi.org/10.1016/j.geomorph.2010.06.011

Chin YP, Aiken G, Loughlin EO (1994) Molecular weight, polydispersity, and spectroscopic properties of aquatic humic substances. Environ Sci Technol 28(11):1853–1858. https://doi.org/10.1021/es00060a015

Conforti M, Buttafuoco G, Leone AP, Aucelli PPC, Robustelli G, Scarciglia F (2013) Studying the relationship between water-induced soil erosion and soil organic matter using Vis–NIR spectroscopy and geomorphological analysis: a case study in southern Italy. Catena 110:44–58. https://doi.org/10.1016/j.catena.2013.06.013

Coplen TB (2011) Guidelines and recommended terms for expression of stable-isotope-ratio and gas-ratio measurement results. Rapid Commun Mass Spectrom 25(17):2538–2560. https://doi.org/10.1002/rcm.5129

Craine JM, Brookshire ENJ, Cramer MD, Hasselquist NJ, Koba K, Marin-Spiotta E, Wang L (2015) Ecological interpretations of nitrogen isotope ratios of terrestrial plants and soils. Plant Soil 396(1–2):1–26. https://doi.org/10.1007/s11104-015-2542-1

De Clercq T, Heiling M, Dercon G, Resch C, Aigner M, Mayer L, Mao Y, Elsen A, Steier P, Leifeld J, Merckx R (2015) Predicting soil organic matter stability in agricultural fields through carbon and nitrogen stable isotopes. Soil Biol Biochem 88:29–38. https://doi.org/10.1016/j.soilbio.2015.05.011

Dijkstra P, Ishizu A, Doucett R, Hart SC, Schwartz E, Menyailo OV, Hungate BA (2006) C-13 and N-15 natural abundance of the soil microbial biomass. Soil Biol Biochem 38(11):3257–3266. https://doi.org/10.1016/j.soilbio.2006.04.005

Doetterl S, Berhe AA, Nadeu E, Wang Z, Sommer M, Fiener P (2016) Erosion, deposition and soil carbon: a review of process-level controls, experimental tools and models to address C cycling in dynamic landscapes. Earth-Sci Rev 154:102–122. https://doi.org/10.1016/j.earscirev.2015.12.005

Dövényi Z (ed) (2010) Inventory of microregions in Hungary. MTAFKI, Budapest (in Hungarian)

Esfahani MR, Stretz HA, Wells MJM (2015) Abiotic reversible self-assembly of fulvic and humic acid aggregates in low electrolytic conductivity solutions by dynamic light scattering and zeta potential investigation. Sci Total Environ 537:81–92. https://doi.org/10.1016/j.scitotenv.2015.08.001

Farsang A, Kitka G, Barta K, Puskás I (2012) Estimating element transport rates on sloping agricultural land at catchment scale (Velence Mts., NW Hungary). Carpath J Earth Environ Sci 7(4):15–26

Fiener P, Dlugoß V, Van Oost K (2015) Erosion-induced carbon redistribution, burial and mineralisation—is the episodic nature of erosion processes important? Catena 133:282–292

Freyer HD, Aly AIM (1974) Nitrogen 15 variations in fertilizer nitrogen. J Environ Qual 3(4):405–406. https://doi.org/10.2134/jeq1974.00472425000300040023x

Guillaume T, Damris M, Kuzyakov Y (2015) Losses of soil carbon by converting tropical forest to plantations: erosion and decomposition estimated by $\delta^{13}C$. Glob Chang Biol 21(9):3548–3560. https://doi.org/10.1111/gcb.12907

Gunina A, Kuzyakov Y (2014) Pathways of litter C by formation of aggregates and SOM density fractions: implications from ^{13}C natural abundance. Soil Biol Biochem 71:95–104. https://doi.org/10.1016/j.soilbio.2014.01.011

Hadi G (2006) Maize varieties in Eastern Central Europe in the first decades of the 20th century. Acta Agronomica Hungarica 54(1):69–82. https://doi.org/10.1556/AAgr.54.2006.1.7

Handley LL, Raven JA (1992) The use of natural abundance of nitrogen isotopes in plant physiology and ecology. Plant Cell Environ 15(9):965–985. https://doi.org/10.1111/j.1365-3040.1992.tb01650.x

Her N, Amy G, Sohn J, Gunten U (2008) UV absorbance ratio index with

size exclusion chromatography (URI-SEC) as an NOM property indicator. J Water Supply Res Technol AQUA 57(1):35–44. https://doi.org/10.2166/aqua.2008.029

Hu Y, Kuhn NJ (2016) Erosion-induced exposure of SOC to mineralization in aggregated sediment. Catena 137:517–525. https://doi.org/10.1016/j.catena.2015.10.024

IUSS Working Group WRB (2015) World reference base for soil resources 2014, update 2015 international soil classification system for naming soils and creating legends for soil maps. World Soil Resources Reports No. 106. FAO, Rome

Jakab G, Kertész Á (2014) Does soil erosion sequestrate soil organic carbon? In: Halldórsson G, Bampa F, Þórsteinsdóttir AB, Sigurdsson BD, Montanarella L, Arnalds A (eds) Soil carbon sequestration for climate food security and ecosystem services: Proceedings of the International Conference 27-29 May 2013 Reykjavik Iceland. Publications Office of the European Union, Luxembourg, pp 233–238

Jakab G, Szabó J, Szalai Z, Mészáros E, Madarász B, Centeri C, Szabó B, Németh T, Sipos P (2016) Changes in organic carbon concentration and organic matter compound of erosion-delivered soil aggregates. Environ Earth Sci 75(2):1–11

Jankauskas B, Fullen MA (2002) A pedological investigation of soil erosion severity on undulating land in Lithuania. Can J Soil Sci 82(3):311–321. https://doi.org/10.4141/S01-058

Kerley SJ, Jarvis SC (1997) Variation in 15N natural abundance of soil, humic fractions and plant materials in a disturbed and an undisturbed grassland. Biol Fertil Soils 24(2):147–152. https://doi.org/10.1007/s003740050223

Kerley SJ, Jarvis SC (1999) The use of 15N natural abundance variation to examine plant and soil organic fractions in pasture under different management practices. Biol Fertil Soils 29(2):135–140. https://doi.org/10.1007/s003740050535

Koba K, Isobe K, Takebayashi Y, Fang YT, Sasaki Y, Saito W, Yoh M, Mo

J, Liu L, Lu X, Zhang T, Zhang W, Senoo K (2010) Delta 15N of soil N and plants in a N-saturated, subtropical forest of southern China. Rapid Commun Mass Spectrom 24(17):2499–2506. https://doi.org/10.1002/rcm.4648

Konert M, Vandenberghe J (1997) Comparison of laser grain size analysis with pipette and sieve analysis: a solution for the underestimation of the clay fraction. Sedimentol 44(3):523–535. https://doi.org/10.1046/j.1365-3091.1997.d01-38.x

Kononova MM (1966) Soil organic matter: its nature, its role in soil formation and in soil fertility, 2nd edn. Pergamon Press, Oxford

Kreitler CW, Ragone SE, Katz BG (1978) N^{15} / N^{14} ratios of ground-water nitrate, Long Island, New York. Ground Water 16(6):404–409. https://doi.org/10.1111/j.1745-6584.1978.tb03254.x

Kuhn NJ, Armstrong EK, Ling AC, Connolly KL, Heckrath G (2012) Interrill erosion of carbon and phosphorus from conventionally and organically farmed Devon silt soils. Catena 91:94–103. https://doi.org/10.1016/j.catena.2010.10.002

Laceby JP, Olley J, Pietsch TJ, Sheldon F, Bunn SE (2015) Identifying subsoil sediment sources with carbon and nitrogen stable isotope ratios. Hydrol Process 29(8):1956–1971. https://doi.org/10.1002/hyp.10311

Lal R, Pimentel D, Van Oost K, Six J, Govers G, Quine T, De Gryze S (2008) Soil erosion: a carbon sink or source? Science 319(5866):1040–1042. https://doi.org/10.1126/science.319.5866.1040

Lehmann J, Kleber M (2015) The contentious nature of soil organic matter. Nature 528(7580):60–68. https://doi.org/10.1038/nature16069

Levin I, Schuchard J, Kromer B, Münnich KO (1989) The continental European Suess effect. Radiocarbon 31(3):431–440. https://doi.org/10.1017/S0033822200012017

Liang BC, Mackenzie AF, Gregorich EG (1999) Changes in ^{15}N abundance and amounts of biologically active soil nitrogen. Biol Fertil Soils 30(1-2):69–74. https://doi.org/10.1007/s003740050589

Mabit L, Benmansour M, Walling DE (2008) Comparative advantages and limitations of the fallout radionuclides 137Cs, 210Pbex and 7Be for assessing soil erosion and sedimentation. J Environ Radioact 99(12):1799–1807. https://doi.org/10.1016/j.jenvrad.2008.08.009

Mie G (1908) Beiträge zur Optik trüber Medien, speziell kolloidaler Metallösungen. Leipzig, Annalen der Physik 330(3):377–445 (in German). https://doi.org/10.1002/andp.19083300302

Mukundan R, Radcliffe DE, Ritchie JC, Risse LM, McKinley RA (2010) Sediment fingerprinting to determine the source of suspended sediment in a southern Piedmont stream. J Environ Qual 39(4):1328–1337. https://doi.org/10.2134/jeq2009.0405

Nottingham AT, Turner BL, Stott AW, Tanner EVJ (2015) Nitrogen and phosphorus constrain labile and stable carbon turnover in lowland tropical forest soils. Soil Biol Biochem 80:26–33. https://doi.org/10.1016/j.soilbio.2014.09.012

Novara A, La Mantia T, Rühl J, Badalucco L, Kuzyakov Y, Gristina L, Laudicina VA (2014a) Dynamics of soil organic carbon pools after agricultural abandonment. Geoderma 235-236:191–198. https://doi.org/10.1016/j.geoderma.2014.07.015

Novara A, Pereira P, Santoro A, Kuzyakov Y, La Mantia T (2014b) Effect of cactus pear cultivation after Mediterranean maquis on soil carbon stock, $d^{13}C$ spatial distribution and root turnover. Catena 118:84–90. https://doi.org/10.1016/j.catena.2014.02.002

Novara A, Cerdà A, Dazzi C, Lo Papa G, Santoro A, Gristina L (2015) Effectiveness of carbon isotopic signature for estimating soil erosion and deposition rates in Sicilian vineyards. Soil Tillage Res 152:1–7

Pansu M, Gautheyrou J (2006) Handbook of soil analysis. Mineralogical, organic and inorganic methods. Springer, Berlin

Parras-Alcántara L, Lozano-García B, Brevik EC, Cerdá A (2015) Soil organic carbon stocks assessment in Mediterranean natural areas: a comparison of entire soil profiles and soil control sections. J Environ Manag 155:219–228. https://doi.org/10.1016/j.jenvman.2015.03.039

Poesen J (2015) Soil erosion hazard and mitigation in the Euro-Mediterranean region: do we need more research? Hungarian Geog Bull 64(4):293–299. https://doi.org/10.15201/hungeobull.64.4.3

Polyakov VO, Lal R (2008) Soil organic matter and CO_2 emission as affected by water erosion on field runoff plots. Geoderma 143(1-2):216–222. https://doi.org/10.1016/j.geoderma.2007.11.005

Schneckenberger K, Kuzyakov Y (2007) Carbon sequestration under Miscanthus in sandy and loamy soils estimated by natural ^{13}C abundance. J Plant Nutr Soil Sci 170(4):538–542. https://doi.org/10.1002/jpln.200625111

Snider DM, Wagner-Riddle C, Spoelstra J (2017) Stable isotopes reveal rapid cycling of soil nitrogen after manure application. J Environ Qual 46(2):261–271. https://doi.org/10.2134/jeq2016.07.0253

Stevenson BA, Kelly EF, McDonald EV, Busacca AJ (2005) The stable carbon isotope composition of soil organic carbon and pedogenic carbonates along a bioclimatic gradient in the Palouse region, Washington State, USA. Geoderma 124(1-2):37–47. https://doi.org/10.1016/j.geoderma.2004.03.006

Suess HE (1955) Radiocarbon concentration in modern wood. Science 122(3166):415–417. https://doi.org/10.1126/science.122.3166.415-a

Szabó J, Jakab G, Szabó B (2015) Spatial and temporal heterogeneity of runoff and soil loss dynamics under simulated rainfall. Hungarian Geog Bull 64(1):25–34. https://doi.org/10.15201/hungeobull.64.1.3

Szabó J, Szabó B, Szalai Z, Ringer M, Jakab G (2017) Runoff and infiltration—case study of a Cambisol. Columella 4:127–130

Szalai Z, Szabó J, Kovács J, Mészáros E, Albert G, Centeri C, Szabó B, Madarász B, Zacháry D, Jakab G (2016) Redistribution of soil organic carbon triggered by erosion at field scale under subhumid climate, Hungary. Pedosphere 26(5):652–665. https://doi.org/10.1016/S1002-0160(15)60074-1

Tan KH (2003) Humic matter in soil and the environment principles and

controversies. Marcel Dekker Inc, New York. https://doi.org/10.1201/9780203912546

Tiessen H, Karamanos RE, Stewart JWB, Selles F (1984) Natural nitogen-15 abundance as an indicator of soil organic matter transformations in native and cultivated soils. Soil Sci Soc Am J 48(2):312–315. https://doi.org/10.2136/sssaj1984.03615995004800020017x

Van Oost K, Quinie TA, Govers G, De Gryze S, Six J, Harden JW, Ritchie JC, McCarty GW, Heckrath G, Kosmas C, Giraldez JV, Marques da Silva JR, Merckx R (2007) The impact of agricultural soil erosion on the global carbon cycle. Science 318(5850):626–629. https://doi.org/10.1126/science.1145724

Vanwalleghem T, Bork HR, Poesen J, Dotterweich M, Schmidtchen G, Deckers J, Scheers S, Martens M (2006) Prehistoric and Roman gullying in the European loess belt: a case study from central Belgium. The Holocene 16(3):393–401. https://doi.org/10.1191/0959683606hl935rp

Vázquez CF, Prieto SG, Cortizas AM, Boado FC (2015) Deciphering the evolution of agrarian technologies during the last ~1600 years using the isotopic fingerprint ($\delta^{13}C$, $\delta^{15}N$) of a polycyclic terraced soil. Estudos do Quaternário, 12, APEQ, Braga, pp 39-53

Viscarra Rossel RA, Walvoort DJJ, McBratney AB, Skjemstad JO (2006) Visible, near infrared, mid infrared or combined diffuse reflectance spectroscopy for simultaneous assessment of various soil properties. Geoderma 131(1–2):59–75. https://doi.org/10.1016/j.geoderma.2005.03.007

Vitorello VA, Cerri CC, Victória RL, Andreux F, Feller C (1989) Organic matter and natural carbon-13 distribution in forested and cultivated Oxisols. Soil Sci Soc Am J 53(3):773–778. https://doi.org/10.2136/sssaj1989.03615995005300030024x

Wang Z, Govers G, Steegen A, Clymans W, Van den Putte A, Langhans C, Merckx R, Van Oost K (2010) Catchment-scale carbon redistribution and delivery by water erosion in an intensively cultivated area. Geomorphology 124(1-2):65–74. https://doi.org/10.1016/j.geomorph.2010.08.010

Wang A, Fang YT, Chen DX, Koba K, Makabe A, Li YD, Luo TS, Yoh M (2014) Variations in nitrogen-15 natural abundance of plant and soil systems in four remote tropical rainforests, southern China. Oecologia 174(2):567–580. https://doi.org/10.1007/s00442-013-2778-5

Watteau F, Villemin G, Bartoli F, Schwartz C, Morel J (2012) 0–20 µm aggregate typology based on the nature of aggregative organic materials in a cultivated silty topsoil. Soil Biol Biochem 46:103–114. https://doi.org/10.1016/j.soilbio.2011.11.021

Werth M, Kuzyakov Y (2010) ^{13}C fractionation at the root–microorganisms–soil interface: a review and outlook for partitioning studies. Soil Biol Biochem 42(9):1372–1384. https://doi.org/10.1016/j.soilbio.2010.04.009

Wynn JG, Harden JW, Fries TL (2006) Stable carbon isotope depth profiles and soil organic carbon dynamics in the lower Mississippi Basin. Geoderma 131(1-2):89–109. https://doi.org/10.1016/j.geoderma.2005.03.005

Yu F, Zong Y, Lloyd JM, Huang G, Leng MJ, Kendrick C, Lamb AL, Yim WWS (2010) Bulk organic δ13C and C/N as indicators for sediment sources in the Pearl River Delta and estuary, southern China. Estuar Coast Shelf Sci 87(4):618–630. https://doi.org/10.1016/j.ecss.2010.02.018

Zhang K, Dang H, Zhang Q, Cheng X (2015) Soil carbon dynamics following land-use change varied with temperature and precipitation gradients: evidence from stable isotopes. Glob Chang Biol 21(7):2762–2772. https://doi.org/10.1111/gcb.12886

Zimmermann M, Leifeld J, Schmidt MWI, Smith P, Fuhrer J (2007) Measured soil organic matter fractions can be related to pools in the RothC model. Eur J Soil Sci 58(3):658–667. https://doi.org/10.1111/j.1365-2389.2006.00855.x

Zollinger B, Alewell C, Kneisel C, Meusburger K, Brandová D, Kubik P, Schaller M, Ketterer M, Egli M (2015) The effect of permafrost on time-split soil erosion using radionuclides (^{137}Cs, $^{239+240}Pu$, meteoric ^{10}Be) and stable isotopes($\delta^{13}C$) in the eastern Swiss Alps. J Soils Sediments 15(6):1400–1419. https://doi.org/10.1007/s11368-014-0881-9